Some properties of multifractality at solid-on-solid growth processes

A. Bershadskii
ICAR, P.O. Box 39953, Ramat-Aviv 61398, Tel-Aviv, Israel
(Received 16 November 1998)

It is shown that multifractality of large deposition probabilities observed in a simple model of crystal growth (the Das Sarma model with neglected surface diffusion, desorption, and hop) corresponds to another type of statistical distribution: multifractal Bernoulli distribution. Lognormal distribution is also discussed in this context. [S1063-651X(99)03606-5]

PACS number(s): 05.40.+a, 81.15.−z, 68.55.−a

I. INTRODUCTION

Simple models of crystal growth turn out to be useful for understanding of some significant properties of this process [1,2]. In the simplest situation we neglect surface diffusion, desorption, and hop, but despite the strong simplification this growth process exhibits multifractal properties [3]. If one takes into account the surface diffusion, desorption, and hop the properties of the multifractal distribution of the growth probability may be changed. However, appearance of the multifractality (as is shown in [3]) can be related to the simplest growth process itself. This process implies such a growth [1,2] that incident atoms are randomly deposited on substrate or on the previous atoms one by one. In this way columns of atoms with various heights appear without vacancies or overhangs. The roughness of the growing surface is characterized by a multifractal distribution [3]. Description of this multifractality can be made as follows.

The two-dimensional substrate with a global size L is divided into boxes of size l and deposition probability of atoms in the box (i,j), $P_{ij}(l/L)$, is defined as

$$P_{ij}(l/L)=\frac{N_{ij}(l/L)}{\sum N_{ij}(l/L)}=\frac{N_{ij}(l/L)}{N},$$

where $N_{ij}(l/L)$ is the number of atoms deposited inside the box (i,j) of size l and N is the total number of deposited atoms.

Partition function

$$Z_q=\sum_{ij}\{P_{ij}(l/L)\}^q\propto(l/L)^{\tau(q)} \tag{1}$$

and the generalized dimensions D_q are defined as

$$D_q=\tau(q)/(q-1). \tag{2}$$

Figure 1 shows the generalized dimensions D_q (against q) obtained in a numerical simulation performed in [3] for average film thickness $h=1$ monolayer (ML) — set II, and for $h=25$ ML — set I. Straight lines in this figure indicate lognormal distribution (see [4] for information about lognormal distribution and its applications and [5,6] for information about multifractality corresponding to lognormal distribution). One can see that lognormal distribution is applicable for $h=1$ ML for positive q up to $q\sim30$. For $q>30$ this distribution transforms into a new one. Since the generalized dimensions with large q are dominated by the boxes (i,j) with large values of the deposition probability $P_{i,j}(l/L)$ (see, for instance, [7]), it is interesting to understand what type of the probability distribution replaces lognormal distribution for the large values of q. It is observed in [3] that with the increasing h the distribution of growth probability tends to be uniform (see, for instance, a set of dots I corresponding to $h=25$ ML in Fig. 1). Closeness of lognormality to homogeneity can also be observed in some natural phenomena [4]. Since D_q is also a function of h it is plausible that this function crosses over continuously between the two limiting behaviors: lognormal and the new one (see also Discussion).

II. MULTIFRACTAL BERNOULLI DISTRIBUTION

Let us define

$$\overline{P}_{ij}=P_{ij}/\max_{ij}\{P_{ij}\}. \tag{3}$$

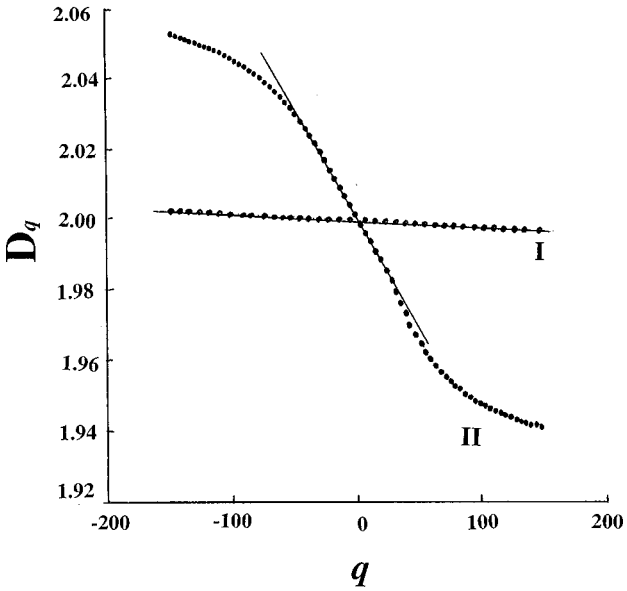

FIG. 1. Generalized dimension spectra D_q against q. Data (dots) are taken from [3]. Set I corresponds to average film thickness $h=25$ ML and set II corresponds to $h=1$ ML. Straight lines indicate lognormal distributions.

Then

$$\langle \overline{P}^q \rangle = \frac{1}{N} \sum_{ij} \overline{P}_{ij}^q . \tag{4}$$

The simplest structure that can be used for fractal description is a system for which $\overline{P}_{ij}$ can take only two values, 0 and 1. It follows from Eqs. (3) and (4) that for such a system (with $q>0$)

$$\langle \overline{P}^q \rangle = \langle \overline{P} \rangle \tag{5}$$

and fluctuations in this system can be identified as Bernoulli fluctuations [8]. It is clear that the Bernoulli fluctuations can be *monofractal* only.

Generalization of Eq. (5) in the form of a generalized scaling

$$\langle \overline{P}^q \rangle \sim \langle \overline{P} \rangle^{g(q)} \tag{6}$$

can be used to describe more complex (multifractal) systems. We use invariance of the generalized scaling (6) with dimension transform [9]

$$\overline{P}_{ij} \to \overline{P}_{ij}^{\lambda} \tag{7}$$

to find $g(q)$. This invariance means that

$$\langle (\overline{P}^{\lambda})^q \rangle \sim \langle (\overline{P}^{\lambda}) \rangle^{g(q)} \tag{8}$$

for all positive λ. Then, it follows from Eqs. (6) and (8) that

$$\langle (\overline{P})^{\lambda q} \rangle \sim \langle \overline{P} \rangle^{g(\lambda q)} \sim \langle \overline{P} \rangle^{g(\lambda) g(q)}. \tag{9}$$

Hence,

$$g(\lambda q) = g(\lambda) g(q). \tag{10}$$

The general solution of functional equation (10) is

$$g(q) = q^{\gamma}, \tag{11}$$

where γ is a positive number. It should be noted that the case $\gamma = 1$ corresponds to Gauss fluctuations [10]. We shall, however, consider the limit $\gamma \to 0$ (i.e., crossover to the Bernoulli fluctuations). This crossover is nontrivial. Indeed, let us consider generalized scaling

$$F_{qm} \sim F_{km}^{\alpha(q,k,m)}, \tag{12}$$

where

$$F_{qm} = \langle \overline{P}^q \rangle / \langle \overline{P}^m \rangle. \tag{13}$$

Substituting Eq. (6) into Eqs. (12) and (13) and using Eq. (11) we obtain

$$\alpha(q,k,m) = \frac{q^{\gamma} - m^{\gamma}}{k^{\gamma} - m^{\gamma}}.$$

Hence,

$$\lim_{\gamma \to 0} \alpha(q,k,m) = \frac{\ln(q/m)}{\ln(k/m)}. \tag{14}$$

If there is ordinary scaling

$$\langle \overline{P}^p \rangle \sim (l/L)^{\zeta_p}, \tag{15}$$

then

$$\alpha(q,k,m) = \frac{\zeta_q - \zeta_m}{\zeta_k - \zeta_m}. \tag{16}$$

From comparing Eqs. (14) and (16) we obtain

$$\frac{\zeta_q - \zeta_m}{\zeta_k - \zeta_m} = \frac{\ln(q/m)}{\ln(k/m)} \tag{17}$$

at the limit $\gamma \to 0$. The general solution of functional equation (17) is

$$\zeta_q = a + c \ln q, \tag{18}$$

where a and c are some constants.

If we use the relationship

$$\max_i \{P_{ij}\} \sim (l/L)^{D_{\infty}} \tag{19}$$

(see, for instance, [7]), then it follows from Eqs. (2), (3) and Eqs. (15), (18), and (19) that

$$D_q = D_{\infty} + c \frac{\ln q}{(q-1)} \tag{20}$$

for the multifractal Bernoulli fluctuations (i.e., for the fluctuations which appear at the limit $\gamma \to 0$).

From Eqs. (6), (15), and (18) we can find $g(q)$ corresponding to the multifractal Bernoulli fluctuations

$$g(q) = 1 + \frac{c}{a} \ln q, \tag{21}$$

where $a = d - D_{\infty}$.

Let us find the characteristic function of the multifractal Bernoulli distribution. It is known that the characteristic function $\chi(\lambda)$ can be represented by the following series (see, for instance, [8]):

$$\chi(\lambda) = \sum_{p=0}^{\infty} \frac{(i\lambda)^p}{p!} \langle \overline{P}^p \rangle. \tag{22}$$

Then using Eqs. (6) and (21) we obtain from Eq. (22)

$$\chi(\lambda) = 1 + \langle \overline{P} \rangle \sum_{p=1}^{\infty} \frac{(i\lambda)^p}{p!} p^{\beta}, \tag{23}$$

where

$$\beta = \frac{c}{(d - D_{\infty})} \ln \langle \overline{P} \rangle. \tag{24}$$

The characteristic function (23) gives a complete description of the multifractal Bernoulli distribution. In the limit $c \to 0$

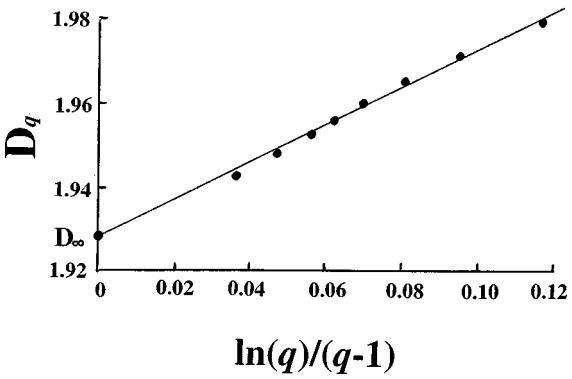

FIG. 2. Generalized dimensions D_q are shown against $\ln(q)/(q-1)$. Data (dots) correspond to set II of Fig. 1 with $q>30$. Straight line is drawn for comparison with the multifractal Bernoulli representation (20).

the characteristic function (23), (24) transforms into a characteristic function of simple Bernoulli distribution [8].

It follows from the definition that $\langle\overline{P}\rangle\leqslant 1$. On the other hand, since $D_q\leqslant D_p$ for $q>p$ it follows from Eq. (20) that $0\leqslant c$. Taking also into account that $D_\infty\leqslant d$ we obtain from Eq. (24) that $\beta\leqslant 0$. This is significant because for $\beta>0$ the representation (23) may not correspond to a normalized probability. Indeed, for this characteristic function $\langle\overline{P}^p\rangle=\langle\overline{P}\rangle p^\beta$. On the other hand, by Hölder inequality one has

$$\langle\overline{P}^p\rangle\leqslant\langle\overline{P}^{pq}\rangle^{1/q}$$

for any integer q. Therefore

$$\langle\overline{P}\rangle p^\beta\leqslant\langle\overline{P}\rangle^{1/q}(pq)^{\beta/q}.$$

Letting q tend to infinity in the above inequality one obtains

$$\langle\overline{P}\rangle p^\beta\leqslant 1.$$

Since $\langle\overline{P}\rangle\leqslant 1$ and $1\leqslant p$ [in representation (24)], then this inequality is satisfied for $\beta\leqslant 0$ and it is not satisfied (for large enough p) when $\beta>0$. Therefore the characteristic function (23) corresponds to some real probability distribution for $\beta\leqslant 0$ only [that takes place in our case, Eq. (24)].

A thermodynamic reason for this restriction can be related to interpretation of c as a specific heat in some multifractal (virtual) thermodynamics (see [11,12]).

III. COMPARISON WITH DATA OF NUMERICAL AND LABORATORY SIMULATIONS

Figure 2 (adapted from [3]) shows the generalized dimensions obtained in the numerical simulation [3] with $h=1$ ML for $q>30$ (cf. Fig. 1). In this figure D_q is shown against $\ln q/(q-1)$. The straight line indicates agreement between the data and the multifractal Bernoulli representation (20). D_∞, shown in this figure, has been obtained using the so-called singularity spectrum $f(\alpha)$ (also calculated in [3]). Thus, one can see that there are two limiting types of growth probability distributions: one (lognormal) corresponds to the boxes with relatively small values of the deposition probability and another (multifractal Bernoulli distribution) corresponds to the boxes with relatively large values of the deposition probability.

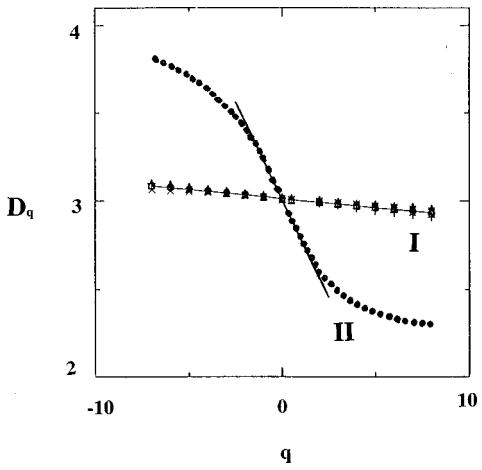

FIG. 3. Generalized dimensions D_q against q. Data (dots) are taken from [16]. Set I corresponds to viscous interval of scales, whereas set II corresponds to convective interval of scales. Straight lines indicate lognormal distributions.

Let us also discuss briefly an analogy with turbulence. Analogy between the growth processes and turbulence was pointed out in papers [9,14,15]. Figure 3 (adapted from [16]) shows generalized dimension spectra obtained in laboratory turbulent flows for a passive scalar dissipation rate. A set of symbols, I, corresponds to the data obtained in so-called viscous interval of scales where the molecular viscosity suppresses the turbulent velocity fluctuations (see also [13]); whereas the set of symbols II corresponds to the data obtained in so-called convective interval of scales where the turbulent fluctuations are fully developed. Straight lines indicate applicability of lognormal distribution. And again (cf. Fig. 1) one can see that for case I (corresponding to suppressed turbulent velocity fluctuations) we have lognormality close to homogeneity, while for case II lognormality takes place only in some vicinity of the point $q=0$. For $q>1$ the multifractality can be described by the multifractal Bernoulli distribution. Indeed, Fig. 4 (obtained from Fig. 3) shows the data corresponding to case II for $q>1$. The straight line indicates agreement between the data (dots) and the multifractal Bernoulli representation (20).

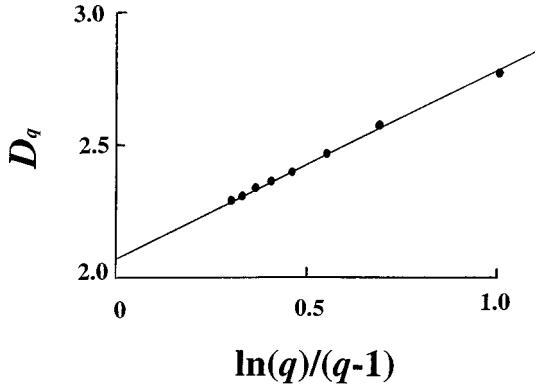

FIG. 4. Generalized dimensions D_q against $\ln(q)/(q-1)$. Data (dots) correspond to set II of Fig. 3 with $q>1$. Straight line indicates agreement with the multifractal Bernoulli representation (20).

Thus, the crossover between these two limiting behaviors of passive scalar turbulent fluctuations seems to be similar to the analogous crossover in the solid-on-solid growth processes. For both these processes lognormal distribution describes relatively small local concentrations, whereas the multifractal Bernoulli distribution describes relatively large local concentrations.

IV. DISCUSSION

Finally, let us discuss briefly some open problems related to the observation represented in this note.

Generally speaking, the observed crossover may turn out to be related to some real transition. To prove this one should show that indeed the behavior of D_q as a function of q is singular at a specific point q_c, as opposed to just crossing over continuously between the two limiting cases. It is known that this is rather difficult to do for such smoothness characteristics as the function D_q is (see, for instance, [17], and references therein). In Fig. 5 we show, as an example, multifractal spectrum D_q of the Hénon attractor as obtained in a recent paper [18] with fuzzy disk counting. In this figure we show both D_q against q (solid curve) and D_q against $\ln q/(q-1)$ (solid circles). The straight line is drawn for comparison with the multifractal Bernoulli representation (20). From theoretical investigations [19] we know that there is a real transition from the ''hyperbolic phase'' to the ''nonhyperbolic phase'' at $q \simeq 2.24$ in this multifractal spectrum. One can assume that the appearance of the multifractal Bernoulli distribution could be an indication of a real transition. However, since in the considered case of the solid-on-solid growth D_q is also a function of h, it is quite plausible that this function simply crosses over continuously between the two limiting cases.

This problem could also be related to the origin of multifractality (cf. [20]) at the growth processes. To discuss this question one must show why this growth has elements of the Bernoulli statistics for large q. This could be shown by mapping the distribution to Bernoulli distribution, and by explaining why this happens in terms of the deposition probabilities. These seem to be interesting problems for future investigations.

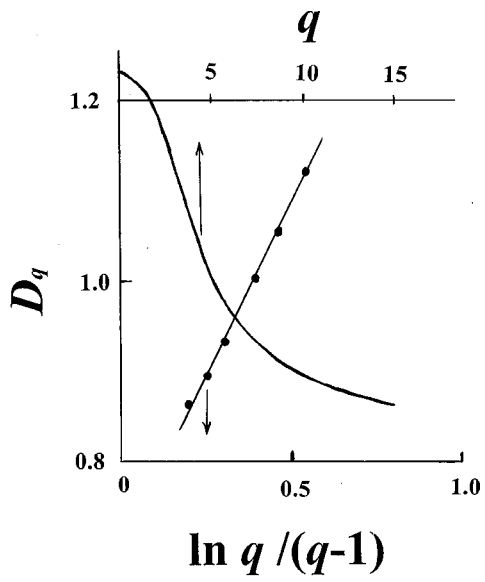

FIG. 5. Generalized dimensions D_q against q (solid curve) and against $\ln(q)/(q-1)$ (solid circles) for the Hénon attractor. Data taken from [18]. Straight line indicates agreement with the multifractal Bernoulli representation (20).

ACKNOWLEDGMENTS

The author is grateful to C.H. Gibson, D. Stauffer, and K.R. Sreenivasan for discussions, and to the Machanaim Center (Jerusalem) for support.

[1] S. Das Sarma, J. Vac. Sci. Technol. A **8**, 2714 (1990).
[2] S. Das Sarma, I.K. Marmorkos, and S.M. Paik, Surf. Sci. **228**, 28 (1990).
[3] W. Bing, W. Yan, and W. Ziqin, Solid State Commun. **96**, 69 (1995).
[4] C.H. Gibson, Proc. R. Soc. London, Ser. A **434**, 149 (1991).
[5] M. Janssen, Int. J. Mod. Phys. B **8**, 943 (1994).
[6] B.L. Altshuler, V.E. Kravtsov, and I.V. Lerner, Phys. Lett. A **134**, 488 (1989).
[7] A. Bershadskii and A. Tsinober, Phys. Lett. A **165**, 37 (1992).
[8] E. Parzen, *Modern Probability Theory and Its Applications* (Wiley, New York, 1967), Sec. 3.
[9] A. Bershadskii, Europhys. Lett. **39**, 587 (1997).
[10] J. Beck and W.W.L. Chen, *Irregularities of Distribution* (Cambridge University Press, Cambridge, England, 1987), Section 1.
[11] H.E. Stanley and P. Meakin, Nature (London) **335**, 405 (1988).
[12] L.D. Landau and E.M. Lifshitz, *Statistical Physics* (Pergamon Press, New York, 1980), Pt. 1.
[13] A. Bershadskii, J. Stat. Phys. **77**, 909 (1994).
[14] J. Krug, Phys. Rev. Lett. **72**, 2907 (1994).
[15] A. Kundagrami, C. Dasgupta, P. Punyindu, and S. Das Sarma, Phys. Rev. E **57**, R3703 (1998).
[16] K.R. Sreenivasan and R.R. Prasad, Physica D **38**, 322 (1989).
[17] A. Arneodo, E. Bacry, and J.F. Muzy, Physica A **213**, 232 (1995).
[18] M. Alber and J. Peinke, Phys. Rev. E **57**, 5489 (1998).
[19] A. Politi, R. Badii, and P. Grassberger, J. Phys. A **21**, L763 (1988).
[20] A. Bershadskii, Phys. Rev. E **55**, 6274 (1997).